Available online at www.sciencedirect.com
ScienceDirect
Journal of Power Sources 161 (2006) 1288–1296
JOURNAL OF POWER SOURCES
www.elsevier.com/locate/jpowsour

Crosslinkable fumed silica-based nanocomposite electrolytes for rechargeable lithium batteries

Yangxing Li, Jeffrey A. Yerian, Saad A. Khan, Peter S. Fedkiw *

Department of Chemical & Biomolecular Engineering, North Carolina State University, Raleigh, NC 27695-7905, USA

Received 28 April 2006; received in revised form 22 May 2006; accepted 6 June 2006
Available online 26 July 2006

Abstract

Electrochemical and rheological properties are reported of composite polymer electrolytes (CPEs) consisting of dual-functionalized fumed silica with methacrylate and octyl groups + low-molecular weight poly(ethylene glycol) dimethyl ether (PEGdm) + lithium bis(trifluoromethanesulfonyl)imide (LiTFSI, lithium imide) + butyl methacrylate (BMA). The role of butyl methacrylate, which aids in formation of a crosslinked network by tethering adjacent fumed silica particles, on rheology and electrochemistry is examined together with the effects of fumed silica surface group, fumed silica weight percent, salt concentration, and solvent molecular weight. Chemical crosslinking of the fumed silica with 20% BMA shows a substantial increase in the elastic modulus of the system and a transition from a liquid-like/flocculated state to an elastic network. In contrast, no change in lithium transference number and only a modest decrease (factor of 2) on conductivity of the CPE are observed, indicating that a crosslinked silica network has minimal effect on the mechanism of ionic transport. These trends suggest that the chemical crosslinks occur on a microscopic scale, as opposed to a molecular scale, between adjacent silica particles and therefore do not impede the segmental mobility of the PEGdm. The relative proportion of the methacrylate and octyl groups on the silica surface displays a nominal effect on both rheology and conductivity following crosslinking although the pre-cure rheology is a function of the surface groups. Chemical crosslinked nanocomposite polymer electrolytes offer significant higher elastic modulus and yield stress than the physical nanocomposite counterpart with a small/negligible penalty of transport properties. The crosslinked CPEs exhibit good interfacial stability with lithium metal at open circuit, however, they perform poorly in cycling of lithium–lithium cells.

Keywords: Electrolyte; Composite gel; Lithium-ion; Crosslinked; Fumed silica

1. Introduction

From electric vehicles to cellular phones, advances in battery technology have not kept pace with the power requirements of these electrical devices. Solid polymer electrolytes are attractive for next-generation lithium batteries since they would overcome limitations of liquid electrolytes for such as: lithium dendrite formation, electrolyte leakage, flammable organic solvent, and electrolytic degradation of electrolyte [1–5]. Although the potential benefits of polymer electrolytes are well recognized, the polymer systems must satisfy demanding material requirements, such as high conductivity (>10^{-3} S cm^{-1} at 25 °C), good mechanical strength, and easy processing. Typically, these properties are mutually exclusive, making optimization of properties difficult.

To date, the most common approaches to solid polymer electrolytes for lithium batteries have employed high-molecular weight ($M_n > 10^5$) polymers based on polyethylene oxide (PEO) [1,6,7]. When combined with lithium salts, linear PEO forms poorly conductive crystalline complexes with room-temperature conductivity <10^{-5} S cm^{-1}, which is too low for practical applications [6,7]. Several strategies have been used to improve the conductivity: the use of flexible polymer chains with low glass-transition temperature, and the addition of liquid plasticizers and solid fillers [8–26]. Adding liquid plasticizers into polymer matrix effectively increases the conductivity by forming a type of gel polymer electrolyte; however, the mechanical properties and stability with lithium metal are poor in the presence of a large fraction of liquid.

* Corresponding author. Tel.: +1 919 515 3572; fax: +1 919 515 3465.
E-mail address: fedkiw@eos.ncsu.edu (P.S. Fedkiw).

0378-7753/$ – see front matter © 2006 Elsevier B.V. All rights reserved.
doi:10.1016/j.jpowsour.2006.06.015

Our group has developed a type of nanocomposite polymer electrolytes (CPEs) with high conductivity and mechanical stability [27–31], consisting of low-molecular weight polyethers + lithium salts + fumed silica. Fumed silica is non-porous SiO_2 prepared by the thermal combustion of silicon tetrachloride in an oxygen–hydrogen flame [32]. The native surface group on fumed silica is silanol (Si–OH), but these may be (partially) replaced by other functional groups [30]. Through hydrogen bonding and/or van der Waals attraction of native or functional surface groups, fumed silica dispersed in a liquid forms a physical gel [28,29,33] that can flow under shear but reforms in the absence of stress [34]. While these physically-interacting fumed silica demonstrate improved interfacial stability of electrolyte with lithium, room-temperature conductivity [29,30,35] exceeding 10^{-3} S cm^{-1}, and reduced dendrite formation [36], the elastic modulus and yield stress of the electrolytes are not sufficient to use without an additional separator. One way to improve the mechanical strength of these composites is to use fumed silica that contains crosslinkable groups on its surface. As a result, the fumed silica network can be made permanent by subsequent reaction, using thermal- or UV-activated initiators, to form covalent rather than physical bonds between adjacent fumed silica.

In a previous communication on crosslinkable fumed silica [37], we have examined the effects of adding crosslinkable monomers to this system, in particular the effects of concentration and alkyl chain length of monomers on conductivity, rheology, and interfacial stability. In this study, we characterize the rheological and electrochemical properties of nanocomposite electrolytes using different types of dual-functionalized, crosslinkable fumed silicas. The effects of fumed silica surface-group ratio (i.e., moles of crosslinkable groups relative to non-reactive octyl groups), fumed silica weight percent, PEGdm molecular weight, and lithium salt concentration on electrochemical and mechanical properties are reported. Since little work has been performed with crosslinkable fumed silica [38], our work represents a unique approach in the design of polymer electrolytes that will provide understanding into how the various components of the crosslinked CPE affect the electrochemical and mechanical properties.

2. Experimental

2.1. Chemicals and preparation of electrolytes

Lithium bis(trifluoromethanesulfonyl)imide (LiTFSI, lithium imide, $LiN(CF_3SO_2)_2$, 3 M) salt is dried at 100 °C under vacuum for several days before use. PEGdm (250 or 500 M_n, Aldrich) is dried over 4 Å molecular sieves for at least 1 week. Commercially available crosslinkable fumed silica (R711, Degussa) is dried at 120 °C for 4 days prior to use. Fumed silica with octyl and methacrylate groups is synthesized by reacting Degussa A200 (hydroxyl surface groups) with octyltrimethoxysilane and trimethoxysilylpropyl methacrylate [38]. This dual-functionalized fumed silica is referred to as TOM *X*:*Y*, where *X* refers to the moles of methacrylate surface groups and *Y* is the moles of octyl surface groups. Three different TOM fumed silicas (TOM 1:4, TOM 1:1, and TOM 4:1) are prepared and characterized [38]. Table 1 shows the surface coverage and basic structure of the TOM silicas. Butyl methacrylate (BMA, Aldrich) monomer is processed through packed columns (Aldrich, 30,631-2) to remove the inhibitor, monomethyl ether hydroquinone (MEHQ), and then stored over molecular sieves at 1 °C. The inhibitor, butylated hydroxytoluene (BHT), in PEGdm (250) is also removed using the same type of column.

The baseline liquid electrolyte is made by dissolving LiTFSI into the PEGdm at a Li:O mole ratio of 1:20 (LiTFSI/PEGdm = 0.323 weight ratio). Composite electrolytes are prepared in an argon-filled glove box by adding appropriate amounts of a solution containing LiTFSI in PEGdm (250) to a known amount of fumed silica. A solution of 1 wt.% 2,2′-azo-bis-isobutylnitrile (AIBN) in monomer is then added to prepare composites with the desired weight percent of monomer. The CPE is mixed by a high-shear mixer (Tissue Tearor, Model 398, BioSpec Products, Inc.) until homogeneous. Samples for rheology measurements are mixed outside the glove box using a Silverson Model SL2 mixer (Silverson Machines). The CPE is then cured in an oven at 80 °C for 24 h in a sealed stainless steel vial to prevent water infusion.

2.2. Characterization of electrolytes

Electrolyte conductivities are measured in a glass cell containing two blocking platinum wire electrodes (0.64-mm diameter, Fisher Scientific) [39]. Conductivity is measured using EG&G Princeton Applied Research PowerSine software to control an EG&G Model 273 potentiostat and an EG&G Model 5210 lock-in amplifier in the frequency range 100 kHz to 100 mHz. Cells are calibrated at 25 °C using a standard KCl solution (1409 μS cm^{-1} at 25 °C). Conductivity cells are placed in wells in an insulated aluminum block with internal coolant circuit connected to a temperature-controlled circulating water bath (Isotope 1016P Fisher Scientific) [31]. The temperature of the water bath is varied from 0 to 100 °C (±1 °C) and the temper-

Table 1
Surface group coverage and type of the TOM (*X*:*Y*) fumed silicas

Crosslinkable fumed silica	Surface coverage[a] (%)	Propyl methacrylate groups *X* (%)	Octyl groups *Y* (%)	Structure
TOM 1:4	50	20	80	octyl group; propyl methacrylate group
TOM 1:1	45	50	50	
TOM 4:1	48	80	20	

[a] Percentage of –OH groups that are modified with octyl or propyl methacrylate groups.

ature of each sample is measured using a T-type thermocouple placed in a sealed glass compartment fully submerged in the sample. For each composition, three to five samples are measured with the reported value representing the average.

The compatibility between electrolyte and lithium metal at room temperature is studied by time-dependent impedance spectroscopy using symmetric lithium/CPE/lithium button cells. The crosslinked CPE is prepared by placing the pre-cured composite in a 1-in. diameter propylene mesh (∼0.3-mm thick, 50% porosity, McMaster-Carr). The CPE/mesh sample is positioned between two Teflon discs to ensure uniform sample thickness, sealed in a stainless vial, and then cured at 80 °C for 24 h. From this CPE/mesh sample, 0.5-in. diameter discs are punched and used in the fabrication of symmetric lithium/CPE/lithium button cells. The impedance of the cell is measured using an EG&G Model 273 potentiostat and an EG&G Model 5210 lock-in amplifier at room temperature. The interfacial resistance between the electrolyte and lithium metal is determined according to the method of Fauteux [40]. For each sample, three cells are prepared and measured. An Arbin battery cycler (Model BT2042) controlled by Arbin ABTS software is employed to carry out constant-current cycling using symmetric lithium/CPE/lithium button cells. In Li/electrolyte/Li cells, current densities of 0.2 mA cm^{-2} with fixed charge density of 1 C cm^{-2} are applied. Cell cycling is terminated upon reaching a cell voltage of 500 mV.

The lithium transference number T_{Li} of the electrolyte is measured using the steady-state current method [41,42]. The impedance of the cell is measured before and after dc-polarization using an EG&G Model 273 potentiostat controlled by EG&G M270 software with an amplitude voltage of 10–50 mV. The cell current is monitored until it reaches steady state. The transference number of each cell is measured about 1 day after fabrication to allow a stable lithium-electrolyte interface to form. Three cells for each sample are measured with the reported value representing the average.

The dynamic rheology of the crosslinked samples is measured using a TA Instruments AR2000 stress-controlled rheometer. Unless otherwise noted, the temperature of the samples is maintained at 25 °C using a Peltier plate. A 20-mm diameter steel parallel-plate fixture with sandpaper adhered to its surface is used on all samples. The sandpaper mitigates the formation of a slip layer, which results in underestimation in the measured properties of the sample [43]. The thickness of the samples ranges from 0.8 to 1.5 mm. Initially, samples are loaded in a manner to maintain a normal force of less than 5 N. At the desired thickness, the normal force is allowed to relax below 3 N prior to measurement. For each sample, a dynamic stress sweep is used to determine the range of stresses within the linear-viscoelastic (LVE) region. A new sample is then loaded and a dynamic frequency sweep (0.01–100 rad s^{-1}) using a pre-determined LVE stress, followed by a dynamic stress sweep at a constant frequency of 1 rad s^{-1} are performed. Reported data represent the average of three measurements, with typical experimental variances less than 20%. The dynamic rheology of the uncrosslinked samples is measured at 25 °C using a DSR stress-controlled rheometer (Rheometrics Scientific) with water-bath temperature control. The measurements are performed using a couette geometry.

A Magna-IR Spectra 750 (Nicolet) spectrometer purged with dry nitrogen is used to acquire absorption spectra by signal averaging 32 scans at a resolution of 4 cm^{-1}. Powder samples are measured by combining the silica (∼2 mg) with 80 mg of KBr and then pressing the powder mixture to 2000 psi using a 12-ton laboratory press (Carver Model C).

3. Results and discussion

3.1. FT-IR of fumed silica

Infrared (IR) studies of the fumed silica were performed to verify the reported surface composition of the TOM silicas and to gain insight on the surface chemistry of the R711 silica. Fig. 1 illustrates the FT-IR spectra (1500–3200 cm^{-1}) of the TOM, R711, R805 (octyl-modified) silicas, and A200 (unmodified) silica in the region of the methacrylate (C=O stretching at ∼1700 cm^{-1}, ν_{st} C=O) and octyl (C–H stretching at 2930 cm^{-1}, ν_{st} C–H) groups. The FT-IR spectrum of A200 lacks peaks in this region which supports that the observed peaks of R805, R711, and TOM are due to octyl and methacrylate groups. The R805 spectrum provides signature peaks for octyl groups at 2930 cm^{-1} that are also present on the TOM silicas. The TOM and R711 spectra exhibit peaks corresponding to octyl and methacrylate groups, which confirms the dual-functionality of these silicas and indicates that R711 has similar surface-functional groups to the TOM silicas even though the exact surface composition is not known. For each silica type, the peak height of Si–O absorbance (∼1100 cm^{-1} not shown in Fig. 1) is used as an internal standard to calculate the relative peak height of the octyl and methacrylate absorbances. Table 2 lists the ratio of the octyl and methacrylate peak heights for the crosslinkable silica. The ratio of absorbances confirms that the relative amount of hydrophobic groups decreases in the following manner: TOM 1:4 > TOM 1:1 > TOM 4:1 > R711.

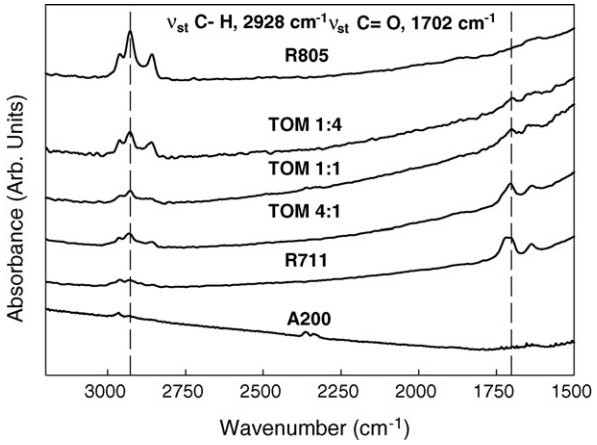

Fig. 1. FT-IR spectra of TOM (*X*:*Y*), R711, R805 (octyl-modified), A200 (unmodified) fumed silica pressed with KBr showing the C–H stretching of octyl group at 2928 cm^{-1} and C=O stretching of methacrylate group at 1702 cm^{-1}. For TOM (*X*:*Y*), *X* refers to the relative number of methacrylate groups and *Y* refers to the relative number of octyl groups.

Table 2
Peak absorbance and peak ratios for the octyl and methacrylate groups on TOM (*X*:*Y*) and R711 silica

Fumed silica	Si–O absorbance (1100 cm^{-1})	Peak ratio Abs_{peak}/Abs_{1100}	
		C=O (1702 cm^{-1})	C–H (2928 cm^{-1})
TOM 1:4	0.947	0.019	0.059
TOM 1:1	1.078	0.021	0.026
TOM 4:1	0.987	0.034	0.029
R711	0.983	0.045	0.015

3.2. Effect of fumed silica surface group on conductivity and rheology

Fig. 2 shows the conductivity of CPEs as a function of temperature for composites with different fumed silica surface groups (R711, TOM 4:1, TOM 1:1, and TOM 1:4) at constant salt concentration and monomer weight percent (20 wt.% BMA). The results indicate that the CPEs have acceptable conductivity and the surface group has a negligible effect on conductivity before crosslinking and a slight effect after crosslinking. Oligomer PEGdm (250) has a relatively low viscosity and hence has a good room-temperature conductivity (>10^{-3} S cm^{-1}) [30,31,44]. Since the conducting phase for LiTFSI is liquid PEGdm in the CPEs systems, the composites present acceptable room-temperature conductivity (>7×10^{-4} S cm^{-1}). These results are consistent with studies using mixtures of oligomeric PEO + non-crosslinkable fumed silica that reveal different surface groups have no significant effect on conductivity [30,35]. The crosslinked systems exhibit about a factor of two reduction in conductivity compared to the non-crosslinked composites. The reduced conductivity of the crosslinked systems is primarily due to a smaller free volume available for ionic transport and not a decrease in polymer segmental mobility. Hou and Baker [38] measured the T_g of PEGdm (500) + $LiClO_4$ electrolytes containing crosslinkable fumed silica and found little or no change in T_g and therefore no decrease in segmental mobility. Because conductivity is a volume-based property, adding crosslinked silica does not significantly decrease the conductivity since there is no strong interaction between PEGdm and silica. The weak dependence of conductivity on the surface group of the silica indicates that the dominant phase for ionic conduction is the bulk PEGdm (250) + LiTFSI electrolyte after crosslinking.

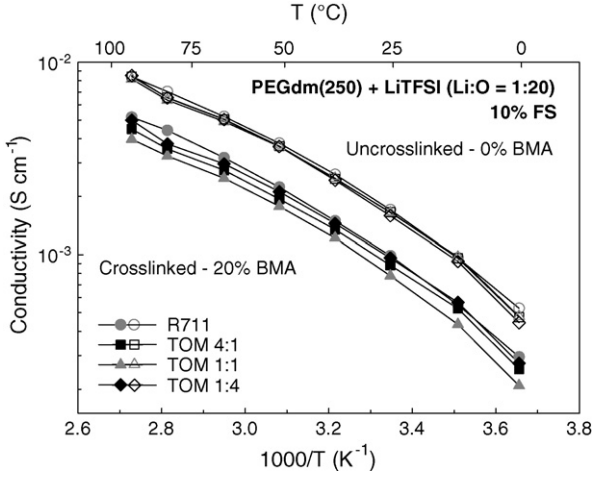

Fig. 2. Conductivity as a function of temperature of crosslinked and uncrosslinked CPEs with three TOM (*X*:*Y*) silicas having different ratios of methacrylate (*X*) to octyl (*Y*) groups on the silica surface and a commercially available crosslinkable silica, R711.

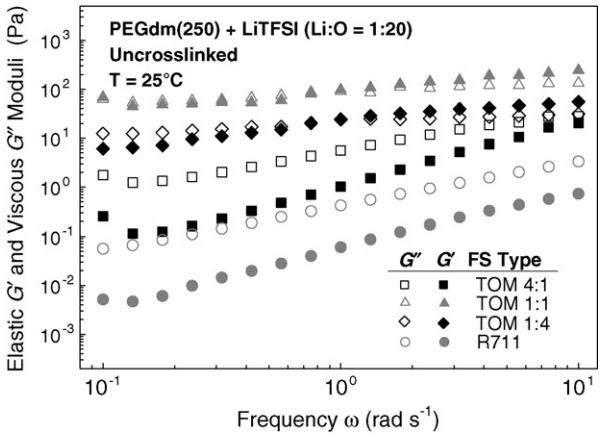

Fig. 3. Effect of crosslinkable fumed silica surface group on elastic and viscous moduli before crosslinking.

The rheological properties of crosslinked CPEs are investigated at constant weight percent of different fumed silicas to determine their role in the microstructure of the composites. Fig. 3 shows the elastic (G') and viscous (G'') moduli as a function of frequency for four different silicas (R711, TOM 4:1, TOM 1:1, and TOM 1:4) before crosslinking. These measurements provide a good indication of the extent of flocculation of the fumed silica prior to crosslinking and show that the samples are more liquid- than solid-like. For uncrosslinked CPEs, G'' exceeds G' at low frequency for all fumed silica types, indicating that the fumed silica is weakly flocculating. Prior to crosslinking, composites containing crosslinkable fumed silica exhibit lower elastic moduli, higher viscous moduli, and greater frequency dependence than conventional fumed silicas that have silanol or octyl surface groups [29,30,35,45]. Degussa R711 and TOM 4:1 exhibits little flocculation, as evident by the higher G'' relative to G' throughout the entire frequency range. Degussa R711 has the lowest G' of the fumed silicas under study primarily due to the fewer number of hydrophobic groups on the silica surface, as determined from FT-IR. While the elastic modulus of the TOM silicas depends on the ratio of the crosslinkable and hydrophobic groups, it did not correlate with the relative amount of hydrophobic groups on the TOM surface. The elastic modulus decreases as TOM 1:1 > TOM 1:4 > TOM 4:1 while the relative hydrophobicity decreases as TOM 1:4 > TOM 1:1 > TOM 4:1. While the lower G' of TOM 4:1 compared to TOM 1:4 and TOM 1:1 may be due to its fewer number of hydrophobic groups, this argument does not hold for the higher G' of TOM 1:1 relative to TOM 1:4.

Fig. 4 shows the elastic modulus as a function of frequency for R711, TOM 4:1, TOM 1:1, and TOM 1:4 fumed silicas after crosslinking. The crosslinked CPEs exhibit gel-like behavior: G' greater G'' and G' relatively independent of frequency. The CPEs containing R711 have the largest G'. The ratio of methacrylate to

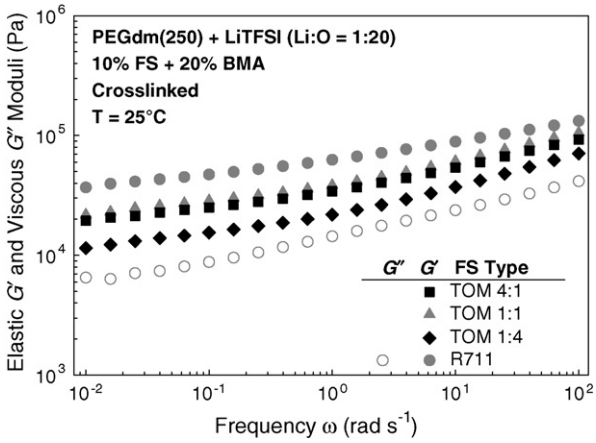

Fig. 4. Effect of crosslinkable fumed silica surface group on dynamic rheology after crosslinking. For clarity, G'' is shown for R711 only but all silicas after crosslinking provide $G' > G''$.

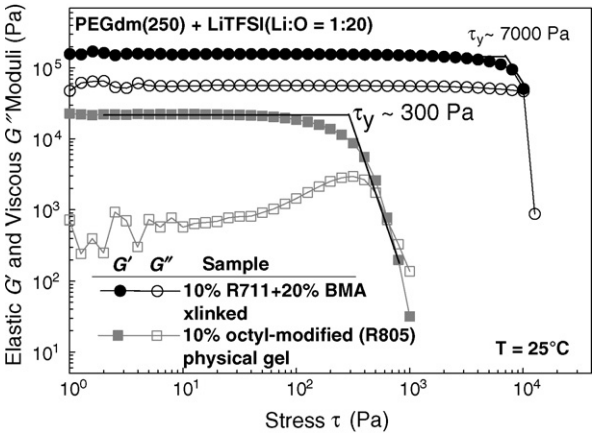

Fig. 5. Comparison of yield stress and moduli for crosslinked (10% R711 + 20% BMA) and non-crosslinked (10% R805) fumed silica composites. Yield stress τ_y is found from intersection of asymptotic regions, as indicated in the figure.

octyl groups of the TOM silicas appears to have a small effect on G'. Samples containing TOM 1:1 and TOM 4:1 have comparable elastic moduli while TOM 1:4 have the lowest G' of the three TOM silicas. The difference in behavior for TOM 1:4 may be due to fewer methacrylate groups on the fumed silica surface which reduces the number of possible covalent crosslinks between the silica particles. TOM 1:4 has only 20% of its groups capable of forming crosslinks compared to 50% and 80% for TOM 1:1 and TOM 4:1, respectively.

The extent of flocculation of the uncrosslinked samples does not correlate with elastic modulus of the crosslinked samples. While electrolytes containing R711 exhibit the lowest G' prior to crosslinking, they have the highest G' after crosslinking. Consequently, the uncrosslinked sample does not need to have a gel-like structure in order to form a gel after crosslinking. This feature is highly desirable for high-volume production of these types of electrolytes since it is more advantageous to process the uncrosslinked samples as liquids and then use photons or heat to cure the electrolytes.

The crosslinked systems exhibit elastic modulus that is several orders of magnitude than that of the uncrosslinked systems, with only a factor of two reduction in conductivity. Furthermore, the crosslinked CPEs have significantly higher yield stress than physical gel electrolytes containing non-crosslinkable (octyl-modified) fumed silica, as illustrated in Fig. 5 [43,46]. In this figure, we have determined the yield stress from the intersection of straight lines drawn through the initial constant region and decreasing part of a plot of elastic modulus versus stress curve. Although other approaches to measuring yield stress exist, this method provides a facile way to examine relative yield stresses [43,46]. The yield stress of the crosslinked CPE is ~7000 Pa with a G' greater than 10^5 Pa compared to a yield stress of ~300 Pa and G' of 2×10^4 Pa for the non-crosslinked physical gel electrolyte. The order of magnitude increase in yield stress and G' for crosslinked CPEs relative to non-crosslinked CPEs is a significant improvement. The crosslinking of conventional filler-free polymer electrolytes can also enhance the elastic modulus and yield stress, but at the expense of reduced conductivity of the electrolytes [47]. The small reduction in conductivity in the crosslinkable fumed silica composites is due to microscopic crosslinking between fumed silica particles rather than molecular crosslinking of the polymer structure, which restricts the segmental mobility. The conductivity and elastic modulus of the crosslinkable fumed silica composites exceed those of conventional crosslinked polymer electrolytes (5×10^{-5} S cm^{-1}) and are comparable to many of the plasticized or gel electrolyte systems [47].

3.3. Effect of fumed silica concentration on conductivity and rheology

Fig. 6 reports the conductivity of crosslinked CPEs as a function of temperature at constant salt content and BMA weight percent, but varying amounts of fumed silica. Increasing the amount of fumed silica results in a decrease in conductivity, a trend observed in other oligomeric PEO systems [28,30,35,45] and is primarily due to a dilution effect. However, as temperature increases above ~75 °C, the relative difference in con-

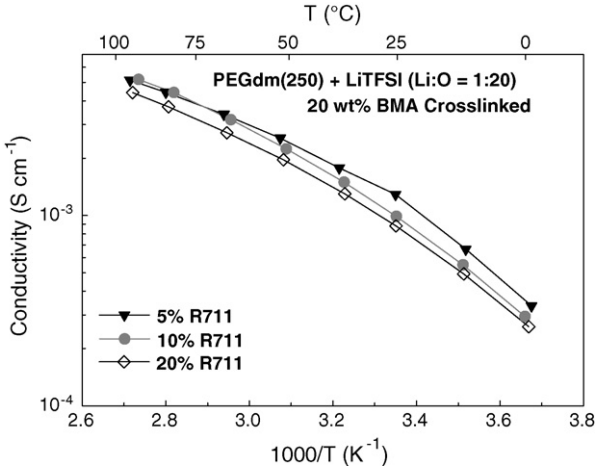

Fig. 6. Effect of R711 weight percent on ionic conductivity after crosslinking as a function of temperature.

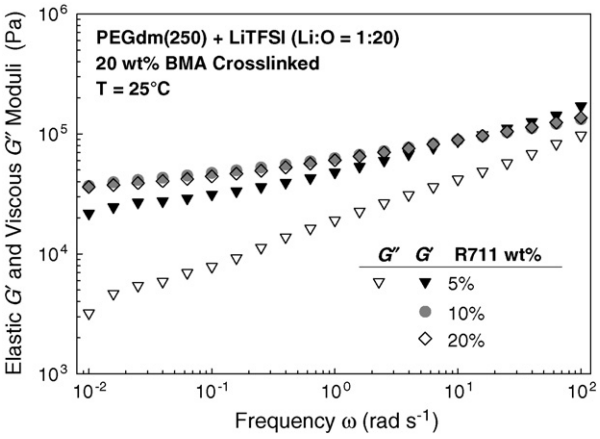

Fig. 7. Effect of R711 weight percent on elastic and viscous moduli after crosslinking.

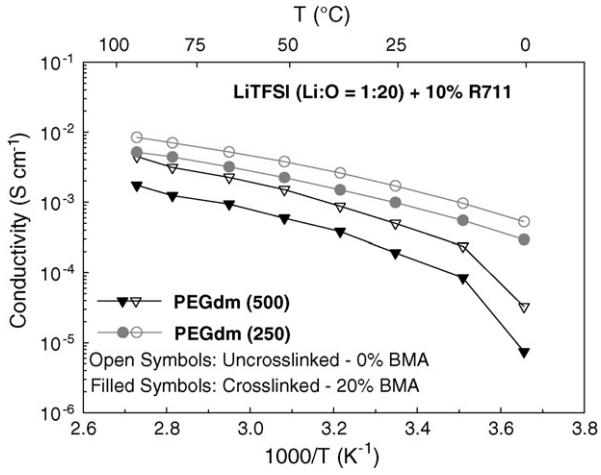

Fig. 8. Effect of PEGdm molecular weight on the ionic conductivity of crosslinked and uncrosslinked composites containing R711 fumed silica.

ductivity between 5% R711 and 10% R711 (or 20% R711) decreases. While this effect is not fully understood, it may be due to polymerized BMA that is not covalently bond to the surface of the silica becoming more soluble in the PEGdm (250) electrolyte with increasing temperature. The solvation of polymerized BMA in the electrolytes increases the viscosity and thus reduces the mobility of the ions.

Fig. 7 shows the elastic and viscous moduli as a function of frequency for varying amounts of R711. The elastic modulus increases slightly at low frequency as fumed silica weight percent increases from 5 to 10 wt.%; however, the elastic modulus does not change upon increase to 20 wt.%. Typically, the elastic modulus of fumed silica gels have been shown to increase in a power-law relationship with fumed silica volume fraction [33,48,49]. At 20 wt.% BMA, the lack of increase in G' with silica concentration for these crosslinked CPEs suggests that the tethering of monomer to the silica surface is the more important factor in dictating the elastic properties, rather than the total volume of fumed silica.

3.4. Effect of PEGdm molecular weight on conductivity and rheology

Fig. 8 reports the conductivity of crosslinked and uncrosslinked composites containing PEGdm (500) or PEGdm (250) and 10% R711. The conductivity of the composites increases as the molecular weight of PEGdm decreases. Furthermore, conductivities of PEGdm (250) and PEGdm (500) crosslinked CPEs exhibit similar dependence on temperature when compared to those of uncrosslinked CPEs. Fig. 9 provides the elastic modulus as a function of frequency for the same systems of PEGdm (250) and PEGdm (500). The higher moduli observed for PEGdm (500) composites may be attributed to the inherently higher viscosity of PEGdm (500) than PEGdm (250) [50]. While the properties of the electrolyte solvent appear to dictate both the ionic transport and rheological properties, more work is needed to understand the role of the solvent in dictating the microstructure of the crosslinkable-based fumed silica composites.

3.5. Effect of crosslinkable fumed silica on lithium transport

Fig. 10 illustrates conductivity versus LiTFSI concentration at 25 and 82 °C for crosslinked CPEs consisting of 10% TOM 1:1 and 20% BMA and their corresponding salt solutions (no fumed silica or monomer). The conductivity of crosslinked composites and uncrosslinked salt solutions follow similar qualitative trends, which suggests that the ionic transport properties of the electrolyte are unaffected by the crosslinked silica network. Furthermore, Fig. 10 shows that the room-temperature conductivity of crosslinked samples is relatively insensitive to salt concentration over the range reported. To further characterize ionic transport in the crosslinked CPEs, the lithium transference number is measured using the method of Bruce and Vincent [42]. Table 3 shows the transference numbers of samples containing 10% TOM 1:1 in a PEGdm (250) + LiTFSI (1:20) electrolyte compared with similar samples that have been crosslinked with 20% BMA. The transference numbers for both systems are comparable (∼0.25) supporting the conclusion that the ionic transport properties in the crosslinked CPEs is not significantly

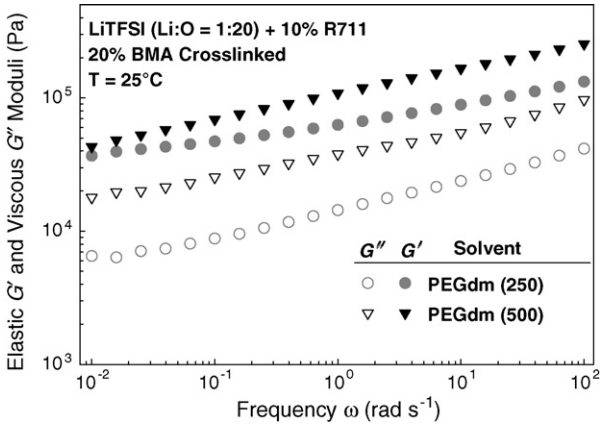

Fig. 9. Effect of PEGdm molecular weight on elastic and viscous moduli of crosslinked composites containing 10 wt.% R711.

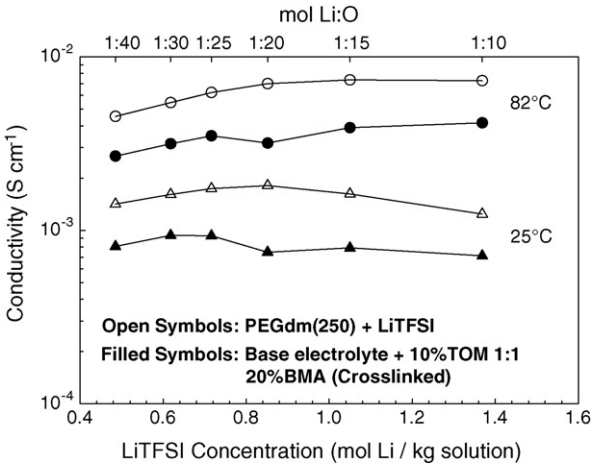

Fig. 10. Effect of LiTFSI concentration on conductivity of crosslinked and uncrosslinked CPEs at 25 and 82 °C.

Table 3
Lithium transference numbers of uncrosslinked and crosslinked composite polymer electrolytes containing 10 wt.% TOM 1:1

Composite CPE	T_{Li} average
PEGdm (250) + LiTFSI (1:20)	0.24 ± 0.03
PEGdm (250) + LiTFSI (1:20) + 10 wt.% TOM 1:1	0.23 ± 0.03
PEGdm (250) + LiTFSI (1:20) + 10 wt.% TOM 1:1 + 20% BMA (1% AIBN) [after crosslinking]	0.21 ± 0.03

affected by the presence of the chemically crosslinked silica network.

3.6. Open-circuit interfacial stability with lithium

The addition of fumed silica stabilizes the interface between lithium metal and salt solutions consisting of PEGdm (250) + LiTFSI (Li:O = 1:20) [24,31,36,45,51]. However, the crosslinked CPEs involves the addition to the electrolyte of monomer and initiator that can also react with lithium metal. Fig. 11 shows the time-dependent interfacial impedance of uncrosslinked composites containing PEGdm (500) + LiTFSI

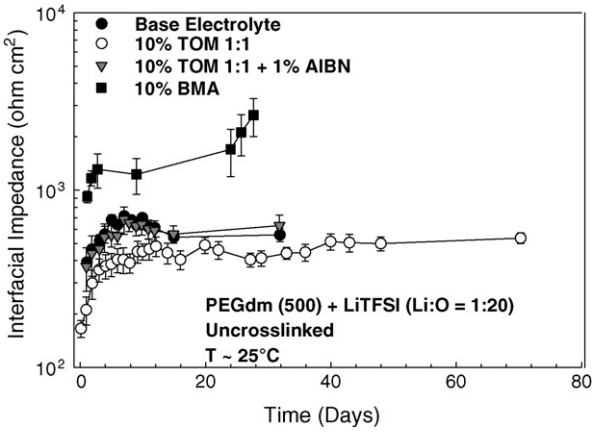

Fig. 11. Time-dependent stability of lithium/CPE interface for uncrosslinked CPEs containing crosslinkable fumed silica, monomer, or initiator.

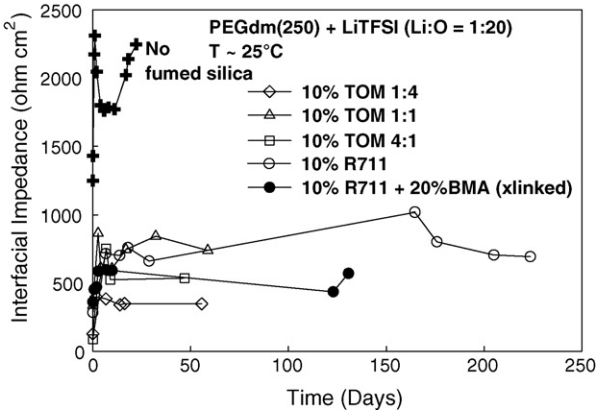

Fig. 12. Open-circuit interfacial stability as a function of time for CPEs containing crosslinkable fumed silica before and after crosslinking. Open symbols represent systems that have not been crosslinked, but contain fumed silica with crosslinkable groups. Closed symbol represent a crosslinked composite electrolyte. The cross symbol represents data for samples without fumed silica [31].

(Li:O = 1:20) and various components involved in the initiation and propagation of the crosslinking reaction: crosslinkable fumed silica (TOM 1:1), monomer (BMA), or initiator (AIBN). The addition of 10 wt.% TOM 1:1 to the base electrolyte improves the interfacial stability, and the presence of an initiator (AIBN) has no effect relative to the base electrolyte. However, addition of BMA produces a CPE/lithium interface with higher impedance compared to the base electrolyte, which suggests that BMA reacts with lithium to form an unstable interface. Although the monomer itself is unstable with respect to lithium, the effect of crosslinked network on compatibility with lithium metal is more important since the concentration of unreacted monomer should be very low after the crosslinking reaction. In addition, the composition of the surface group on the crosslinkable fumed silica may also affect the interfacial stability with lithium. Fig. 12 illustrates the time-dependent open-circuit interfacial impedance of lithium in contact with PEGdm (250) + LiTFSI (Li:O = 1:20) electrolytes that contain crosslinkable-based fumed silica. Results before and after crosslinking indicate that the addition of TOM or R711 crosslinkable fumed silicas (prior to crosslinking) does not produce an unstable interface when compared with electrolyte systems without fumed silica. There is no correlation between interfacial stability and surface group of the fumed silica. Although the degree of stabilization is less than non-crosslinkable silicas [31], such as Degussa R805 or Degussa A200, the methacrylate groups on the silica do appear to be stable with lithium. Previous results have shown that composite electrolytes with higher moduli typically exhibit better interfacial stability [45]. More importantly, addition of 20 wt.% monomer (BMA) and subsequent crosslinking did not result in significant increases in the interfacial impedance. A crosslinked electrolyte comprising 20 wt.% BMA + 10% R711 + PEGdm (250) + LiTFSI (1:20) exhibited better interfacial stability than similar uncrosslinked CPEs. This is promising in that the crosslinked composite may be used with lithium metal despite the use of a highly reactive monomer.

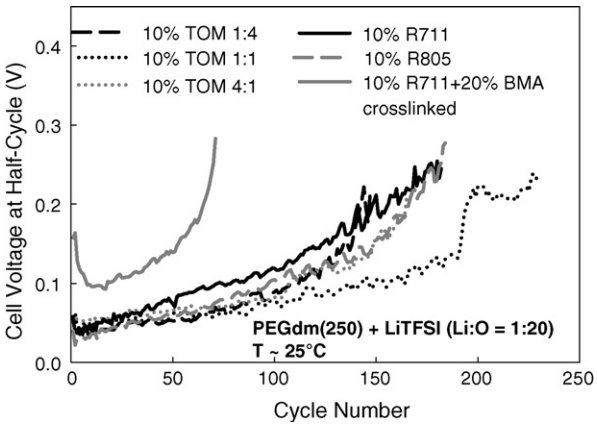

Fig. 13. Average voltage of Li/CPE/Li cells using crosslinkable fumed silica as a function of surface group for both uncrosslinked and crosslinked CPEs.

3.7. Effect of crosslinkable surface group and crosslinked silica network on lithium/lithium cycling

The crosslinkable fumed silica displays relatively good interfacial stability with lithium metal at open-circuit conditions, but the presence of these reactive groups can still pose problems during actual charge/discharge cycles. Fig. 13 illustrates the half-cycle cell voltage versus cycle number for Li/CPE/Li cells containing crosslinkable fumed silica (no monomer or crosslinking) and octyl-modified fumed silica (R805) as a control. The results indicate that the crosslinkable fumed silicas perform equally well in charge/discharge cycles when compared to the octyl-modified systems. The lithium cycling performance, as measured via the cell voltage at half-cycle, is relatively insensitive to the silica surface group. For each silica type, the cell voltage increases with cycle number, with all CPEs being cycled over 140 times before exceeding the cut-off voltage (300 mV). The open-circuit interfacial impedance and the lithium–lithium cycling performance do not appear to correlate. In addition, the crosslinked CPE reaches the cut-off voltage at an earlier cycle number and has a higher voltage compared to the uncrosslinked CPEs. The crosslinked CPE could only be cycled 71 times compared to 182 cycles for the uncrosslinked CPE. Two possible reasons can be posited to explain the lower cycle life of the crosslinked CPE. First, the presence of unstable species, such as unreacted monomer (BMA) or growing polymer, in contact with lithium metal may result in higher voltage. Second, there may also be poor interfacial contact between the electrolyte and lithium metal. The crosslinked electrolytes are robust solids that may not be able to maintain contact with lithium during cycling. Future work is aimed at determining the relative effects of these factors.

4. Summary

Nanocomposite polymer electrolytes containing crosslinkable fumed silica have been successfully prepared and characterized. The surface groups of the crosslinkable fumed silica do not have a significant effect on conductivity before crosslinking and have a slight effect after crosslinking. Crosslinked CPEs have a room-temperature conductivity approaching 10^{-3} S cm^{-1}. Compared to uncrosslinked composites, the conductivity decreases by a factor of two upon crosslinking with 20% BMA, but the elastic modulus of the composites increases several orders of magnitude. The conductivity of the crosslinked CPEs exhibits a similar dependence on temperature when compared to uncrosslinked CPEs, with no change in lithium transference number. Since the crosslinks occur between silica particles, as opposed to polymer, the ionic transport properties of the electrolyte are not affected. The surface groups of the fumed silica significantly affect the rheology of pre-cured composites, but after crosslinking the surface group dependence is weaker. Compared with physical nanocomposite gel electrolytes, chemical crosslinked nanocomposite counterparts offer significant higher elastic modulus and yield stress. The electrolyte solvent plays an important role in dictating both the transport and rheological properties of the composites, with PEGdm (500) composites yielding higher moduli but lower conductivity than PEGdm (250) composites. The crosslinked CPEs exhibit higher cell voltage than uncrosslinked CPEs during cycling of Li/CPE/Li cells possibly due to the presence of residual BMA and/or poor CPE/lithium interfacial contact.

Acknowledgments

The authors gratefully acknowledge funding from the Department of Energy, Office of Basic Energy Sciences and Office of FreedomCar Vehicle Technologies. In addition, we acknowledge the U.S. Department of Education Graduate Assistance in Areas of National Need (GAANN) Fellowship for providing additional funding. We also thank Degussa for providing the fumed silica and 3M for providing the LiTFSI salt. We also acknowledge Dr. Gregory L. Baker and Micah Stowe at Michigan State University for technical discussions and for providing the crosslinkable fumed silica.

References

[1] F.M. Gray, Solid Polymer Electrolytes: Fundamentals and Technological Applications, VCH Press, Cambridge, UK, 1991.
[2] M. Gauthier, A. Belanger, B. Kapfer, G. Vassort, M. Armand, Polymer Electrolyte Reviews, Elsevier Science Publishers, London, UK, 1989.
[3] P.G. Bruce, C.A. Vincent, J. Chem. Soc., Faraday Trans. 89 (1993) 3187.
[4] M. Armand, Solid State Ion. 69 (1994) 309.
[5] H.J. Gores, J.M.G. Barthel, Pure Appl. Chem. 67 (1995) 919.
[6] F.M. Gray, Polym. Elect. (1997).
[7] J.Y. Song, Y.Y. Wang, C.C. Wan, J. Power Sources 77 (1999) 183.
[8] C. Zhang, E. Staunton, Y. Andreev, P.G. Bruce, J. Am. Chem. Soc. 127 (2005) 51.
[9] A.M. Stephan, Eur. Polym. J. 42 (2006) 21.
[10] W. Wieczorek, Z. Florjanczyk, J.R. Stevens, Electrochim. Acta 40 (1995) 2251.
[11] F. Croce, G.B. Appetecchi, L. Persi, B. Scrosati, Nature 394 (1998) 456.
[12] F. Capuano, F. Croce, B. Scrosati, J. Electrochem. Soc. 138 (1918).
[13] J.E. Weston, B.C.H. Steele, Solid State Ion. 7 (1982) 75.
[14] B. Scrosati, J. Electrochem. Soc. 136 (1989) 2774.
[15] J. Plocharski, W. Wieczorek, Solid State Ion. 28 (1988) 979.
[16] F. Croce, B. Scrosati, G. Mariotto, Chem. Mater. 4 (1992) 1134.
[17] W. Gang, J. Roos, D. Brinkmann, F. Capuano, F. Croce, B. Scrosati, Solid State Ion. 53–56 (1992) 1102.

[18] W. Wieczorek, Mater. Sci. Eng. B 15 (1992) 108.
[19] M.C. Borghini, M. Mastragostino, S. Passerini, B. Scrosati, J. Electrochem. Soc. 142 (1995) 2118.
[20] W. Wieczorek, K. Such, Z. Florjanczyk, J.R. Stevens, J. Phys. Chem. 98 (1994) 6840.
[21] F. Croce, S. Passerini, A. Selvaggi, B. Scrosati, Solid State Ion. 40/41 (1990) 375.
[22] W. Wieczorek, K. Such, H. Wycislik, J. Plocharski, Solid State Ion. 36 (1989) 255.
[23] B. Kumar, L.G. Scanlon, Solid State Ion. 124 (1999) 239.
[24] F. Croce, R. Curini, A. Martinelli, L. Persi, F. Ronci, B. Scrosati, R. Caminiti, J. Phys. Chem. B 103 (1999) 10632.
[25] B. Scrosati, F. Croce, L. Persi, J. Electrochem. Soc. 147 (2000) 1718.
[26] G.B. Appetecchi, S. Scaccia, S. Passerini, J. Electrochem. Soc. 147 (2000) 4448.
[27] J. Qiao, Y. Chen, G.L. Baker, Chem. Mater. 11 (1999) 2542.
[28] S.A. Khan, G.L. Baker, S. Colson, Chem. Mater. 6 (1994) 2359.
[29] S.R. Raghavan, M.W. Riley, P.S. Fedkiw, S.A. Khan, Chem. Mater. 10 (1998) 244.
[30] J. Fan, S.R. Raghavan, X.Y. Yu, S.A. Khan, P.S. Fedkiw, J. Hou, G.L. Baker, Solid State Ion. 111 (1998) 117.
[31] J. Fan, P.S. Fedkiw, J. Electrochem. Soc. 144 (1997) 399.
[32] Basic Characteristics of Aerosil, Degussa Technical Bulletin No. 11, Degussa Corp., Akron, OH, 1993.
[33] S.A. Khan, N.J. Zoeller, J. Rheol. 37 (1993) 1225.
[34] S.R. Raghavan, S.A. Khan, J. Rheol. 39 (1995) 1311.
[35] H.J. Walls, J. Zhou, J.A. Yerian, P.S. Fedkiw, S.A. Khan, M.K. Stowe, G.L. Baker, J. Power Sources 89 (2000) 156.
[36] Y.X. Li, P.S. Fedkiw, S.A. Khan, Electrochim. Acta 47 (2002) 3853.
[37] J.A. Yerian, S.A. Khan, P.S. Fedkiw, J. Power Sources 135 (2004) 232.
[38] J. Hou, G.L. Baker, Chem. Mater. 10 (1998) 3311.
[39] M. Riley, P.S. Fedkiw, S.A. Khan, J. Electrochem. Soc. 149 (2002) A667.
[40] D. Fauteux, A. Massucco, M. McLin, M. Vanburen, J. Shi, Electrochim. Acta 40 (1995) 2185.
[41] P.G. Bruce, J. Evans, C.A. Vincent, Solid State Ion. 28 (1988) 918.
[42] P.G. Bruce, C.A. Vincent, J. Electroanal. Chem. 225 (1987) 1.
[43] H.J. Walls, S.B. Caines, A.M. Sanchez, S.A. Khan, J. Rheol. 47 (2003) 847.
[44] K.M. Abraham, Z. Jiang, B. Carroll, Chem. Mater. 9 (1997) 1978.
[45] J. Zhou, P.S. Fedkiw, S.A. Khan, J. Electrochem. Soc. 149 (2002) A1121.
[46] V.B. Pai, S.A. Khan, Carbohyd. Polym. 49 (2002) 207.
[47] W.H. Meyer, Adv. Mater. 10 (1998) 439.
[48] N.B. Uriev, I.Y. Ladyzhinsky, Colloid Surf. A: Physicochem. Eng. Asp. 108 (1996) 1.
[49] H.J. Walls, M.W. Riley, R.R. Gupta, R.J. Spontak, P.S. Fedkiw, S.A. Khan, Adv. Funct. Mater. 13 (2003) 710.
[50] S.R. Raghavan, J. Hou, G.L. Baker, S.A. Khan, Langmuir 16 (2000) 1066.
[51] Y. Fu, X. Ma, Q. Yang, X. Zong, Mater. Lett. 57 (2003) 1759.